Solution Structure of Pituitary Adenylate Cyclase Activating Polypeptide by Nuclear Magnetic Resonance Spectroscopy†

Victor Wray,*,‡ Christel Kakoschke,‡ Kiyoshi Nokihara,§,‖ and Satoru Naruse⊥

Gesellschaft für Biotechnologische Forschung, Mascheroder Weg 1, D-3300 Braunschweig, Germany, Biotechnology Instruments Department, Shimadzu Corporation, Kyoto, 604 Japan, Tokyo University of Agriculture and Technology, Koganei, Tokyo, 184 Japan, and National Institute of Physiological Sciences, Okazaki, 444 Japan

Received November 30, 1992; Revised Manuscript Received February 23, 1993

ABSTRACT: The solution structures of the recently discovered neuropeptides PACAP38 and PACAP27 have been investigated in aqueous solution containing varying amounts of trifluoroethanol (TFE) by circular dichroism (CD) spectroscopy and a combination of 2D ^{1}H nuclear magnetic resonance (NMR) spectroscopy, distance geometry, and refined molecular dynamics and energy minimization calculations. In aqueous solution both peptides show only small transitory amounts of stable structure while in 50% TFE they adopt ordered structures. Qualitative NOE data and the use of the chemical shift index of the α-protons identified the positions of α-helical regions. A set of low-energy conformations compatible with the quantitative NOE data were obtained for both and each set were subjected to RMS analysis to determine the positions of the secondary structure elements. PACAP38 has an initial disordered N-terminal domain of eight amino acids, followed by an α-helical structure stretching from Ser-9 to Val-26, which contains a discontinuity between Lys-20 and Lys-21, and in the C-terminal region there is a short α-helix between Gly-28 and Arg-34. The structure of PACAP27 mirrors remarkably closely that of PACAP38 and shows no fraying of the C-terminal helix. The physiological significance of the three structural domains (1–8, 9–26, and 27–38) of PACAP38 is shown by a comprehensive review of recent *in vitro* and *in vivo* investigations of PACAP analogues. The correspondence of the global structural features of PACAP with other members of this family of peptides (namely, secretin, glucagon, GHRF1–29 and VIP) is demonstrated by inspection of the chemical shift indices of the α-protons.

Since the discovery of the neuropeptide pituitary adenylate cyclase activating polypeptide amide (PACAP)[1] (Miyata et al., 1989), which occurs naturally in two forms consisting of a 38 amino acid peptide amide (PACAP38) and its 27 amino acid N-terminus (PACAP27), considerable attention has been focused on its physiological function (Arimura, 1992). PACAP was first demonstrated in the hypothalamus and later in peripheral tissues, such as the respiratory, genital–urinary, and gastrointestinal systems. It belongs to the secretin/glucagon/vasoactive intestinal peptide (VIP) family and shows the highest homology (68%) with the latter. The high quality synthesis of PACAP, VIP, and several related peptides (Nokihara et al., 1991, 1992) provided sufficient quantities of material for both physiological and structural studies. The failure of such small linear peptides to crystallize suggested that NMR spectroscopy is the method of choice for detailed structural studies.

Ideally, it would be preferable to study the structure of the peptide bound or in equilibrium with the membrane-bound receptor (Schwyzer, 1986). Unfortunately such studies are currently not possible, and both the unavailability of the receptor in sufficient quantities and its high molecular weight [57 000 (Gottschall et al., 1991); 70 000 (Saloman et al., 1992)] prevent NMR studies at present. Hence one must resort to studies of the free hormone in the hope that this will show propensities that are appropriate to the *in vivo* receptor-bound molecule. In contrast to enzymes, with rigid tertiary structures, this type of small molecular weight hormone or neurotransmitter usually shows little evidence of defined stable structure in aqueous solution, and it is necessary to provide an artificial hydrophobic environment that mimicks, as far as possible, the environment in the vicinity of the peptide/receptor interface. This is achieved most conveniently by the use of micelle solutions or aqueous organic solvents, such as methanol or trifluoroethanol (TFE). Under limiting conditions, both media appear to furnish similar structures (Mammi & Peggion, 1990; Motta et al., 1991), and hence, for convenience, we have used aqueous TFE. Although the use of this solvent can be criticized, it is reasonable to believe that in small peptides it stabilizes helices in only those regions of the peptide that have a propensity for helical structure and leaves untouched, as flexible regions, those parts of the peptide that have no such preference (Sönnichsen et al., 1992).

As an extension of our synthetic and physiological studies of PACAP, VIP, and related peptides we present here details of the solution structure of PACAP38 and PACAP27 and show their correspondence to other members of the family and the relationship to their known biological properties.

† This work was supported by the Monbusho International Scientific Research Programme of the Ministry of Education, Science and Culture, Japan.

‡ Gesellschaft für Biotechnologische Forschung.

§ Shimadzu Corp.

‖ Tokyo University of Agriculture and Technology.

⊥ National Institute of Physiological Sciences.

[1] Abbreviations: 1D, one dimensional; 2D, two dimensional; CD, circular dichroism; COSY-DQF, double-quantum filtered correlation spectroscopy; GB, Gaussian line broadening; GHRF(1–29), growth hormone release factor residues 1–29; HPLC, high-performance liquid chromatography; LB, Lorenzian line broadening; NMR, nuclear magnetic resonance; NOE, nuclear Overhauser enhancement; NOESY, nuclear Overhauser enhancement and exchange spectroscopy; PACAP, pituitary adenylate cyclase activating polypeptide C-terminal amide; PACAP38 and PACAP27, pituitary adenylate cyclase activating polypeptide C-terminal amide residues 1–38 and 1–27, respectively; RMS, root mean square; TFA, trifluoroacetic acid; TFE, 2,2,2-trifluoroethanol; TMS, tetramethylsilane; TOCSY, total correlation spectroscopy; VIP, vasoactive intestinal peptide.

0006-2960/93/0432-5832$04.00/0

MATERIALS AND METHODS

Peptide Synthesis. PACAP27 and PACAP38 were efficiently synthesized (Nokihara et al., 1992) by the Fmoc strategy using a novel simultaneous solid-phase peptide synthesizer, Shimadzu PSSM-8 Peptide Synthesizer (Shimadzu, Kyoto, Japan). Using TentaGel SRAM resin (Rapp Polymer, Tübingen, Germany), each Fmoc amino acid was incorporated by activation with PyBOP (Novabiochem AG, Läfelingen, Switzerland) with 1-hydroxybenzotriazole in the presence of *N*-methylmorpholine. After assembly of the desired peptides, the resulting protected peptide resin was cleaved with TFA containing scavengers. The resulting crude peptides, which showed almost 90% purity on reverse-phase HPLC, were easily purified by a single-step preparative HPLC. The homogeneity of the purified peptides were confirmed by fast atom bombardment mass spectrometry, amino acid analysis, and sequencing as demonstrated previously (Nokihara et al., 1992).

Sample Preparation, CD, and NMR Spectroscopy. CD spectra were recorded at room temperature on a Jasco J-600 spectropolarimeter (Jasco, Tokyo, Japan) interfaced to a Commodore PC40-40 (Commodore, Braunschweig, Germany). Samples of each peptide were dissolved in the appropriate mixtures of TFE/H_2O without buffer at concentrations of 0.1 mg mL^{-1}. CD data, measured at wavelengths between 182 and 264 nm, were quantified, in terms of the various secondary structure elements present, by the use of the program VARSELEC (Hennessey & Johnson, 1981; Johnson, 1990), which used data in the range 184–260 nm and can be expected to give statistically meaningful estimates of several types of secondary structure (Johnson, 1990).

Samples of PACAP27 (3.7 mg) and PACAP38 (6 mg) for NMR measurements were dissolved in 0.3 mL of H_2O and 0.3 mL of TFE-d_2 [produced by fractional distillation of a 1:1 (v/v) mixture of H_2O and TFE-d_3 (Merck, Darmstadt, Germany)]. There was no reason to believe, from the NMR results below, that at these concentrations the peptides were aggregated. All spectra were referenced to the residual signal of the methylene protons of TFE at 3.95 ppm relative to TMS. Initial NMR measurements with the same sample of PACAP27 were taken in 9:1 (v/v) H_2O/D_2O.

All 1D and 2D ^1H NMR spectra were recorded at 300 K on a Bruker AM 600 NMR spectrometer, using a dedicated 5-mm proton probe head with external temperature control (Haake GmbH, Karlsruhe, Germany), locked to the deuterium resonance of the solvent and without spinning. 2D experiments [COSY-DQF (Rance et al., 1983), TOCSY in the "CLEAN" mode with the MLEV-17 mixing sequence without trim pulses (Griesinger et al., 1988), and NOESY (Jeener et al., 1979; Macura et al., 1981)] were carried out in the phase-sensitive mode with time-proportional phase increments (Redfield & Kunz, 1975) using standard Bruker software. Low-power irradiation of the water signal, with O1/O2 phase coherence (Zuiderweg et al., 1986), was performed during the relaxation delay (1 and 3 s for TOCSY and NOESY, respectively) and during the mixing time of the NOESY experiments. The mixing times for the TOCSY spectra were 70 ms and the corresponding ones for the NOESY spectra were 150 ms for PACAP27 and 50, 100, 150, and 200 ms for PACAP38. Nomally 512 t_1 increments were sampled with 2K data points over a 7812.5-Hz spectral width and 80 scans per increment. Prior to Fourier transformation, FID's were multiplied by a Gaussian window function (*LB* −20 and *GB* +0.1) in the f_2 domain and a quadratic sine-bell window function, shifted by $\pi/6$, in the f_1 domain. Data processing was performed on a Bruker Aspect X32 data station operating under UNIX. Cross peaks in the NOESY spectra were identified, located, and integrated by the use of the program AURELIA (Neidig & Kalbitzer, 1990).

Structure Calculations. The volumes of the integrated NOESY cross peaks, from the NOESY spectra recorded with mixing times of 150 ms, were calibrated against the known distance (0.197 nm) of the geminal protons of the C-terminal amide and grouped into five categories corresponding to upper distance limits of 0.25, 0.28, 0.32, 0.36, and 0.43 nm. Corrections for pseudoatoms and methyl groups were applied where appropriate. Initially, distance geometry calculations with the program DISGEO (Havel & Wüthrich, 1984) were performed on a VAX 3100/76 station operating under VMS 5.50 (Digital Co., Maynard, MA). Initial structures were created without embedding of intermediate substructures, and the metrization step was replaced by filling in the initial distance matrix with uncorrelated random numbers between the geometrically allowed bounds. Structures from the DISGEO calculations were accepted for subsequent refinement when there was no distance violation greater than 0.04 nm and total error function greater than 3.1 for PACAP27, and 0.10 nm and 3.4, respectively, for PACAP38.

In the next step, the best distance geometry structures were subjected to energy minimization and molecular dynamics simulations using the program XPLOR version 1.5 (Brünger et al., 1986) on a TRACE minisupercomputer (GEI, Aachen, Germany) with UNIX as operating system. The NOE's were incorporated as upper limits for the distances between specific pairs of protons using a semiharmonic extrapotential. The following protocol was used: Initially 500 steps of restrained energy minimization were run to relieve some inherent strain and bad van der Waals contacts. A harmonic potential with a force constant of 210 kJ·nm^{-2}·mol^{-1} was used for the distance restraints. Next, as an equilibrium stage, the structure was subjected to restrained molecular dynamics for 0.05 ps with the initial velocity assignment corresponding to a temperature of 300 K using the same force constant. This was followed by restrained molecular dynamics at 1000 K for 8 ps in which the force constant doubled every 0.5 ps to the final value of 13 440 kJ·nm^{-2}·mol^{-1}, which was used for the rest of the calculation. After 0.5 ps of dynamics at 600 K and 0.5 ps at 300 K, 500 steps of restrained energy minimisation were performed to produce a final structure. Two or more different random seeds for initial velocity assignments per DISGEO structure were used in order to give a representative number of final refined structures. These were accepted for final statistical analysis when the value of the total potential energy was less than −1450 kJ mol^{-1} and the energy contribution associated with distance restraint violations did not exceed a threshold value of 30.4 kJ mol^{-1} for PACAP27, and −2500 and 80.8 kJ mol^{-1} for PACAP38, respectively. The final refined structures were displayed and manipulated on a Hewlett-Packard graphics station using the program BRAGI (Schomburg & Reichelt, 1988), which also allowed calculation of the RMS deviations between structures.

RESULTS

On the addition of TFE to aqueous solutions of either PACAP27 or PACAP38 the shape of the CD curves became increasingly characteristic of α-helical secondary structure (Figure 1). The initial shallow curves in 0% TFE became more pronounced on the addition of TFE with the minimum absorption at ca. 200 shifting to 206 nm, and a second negative

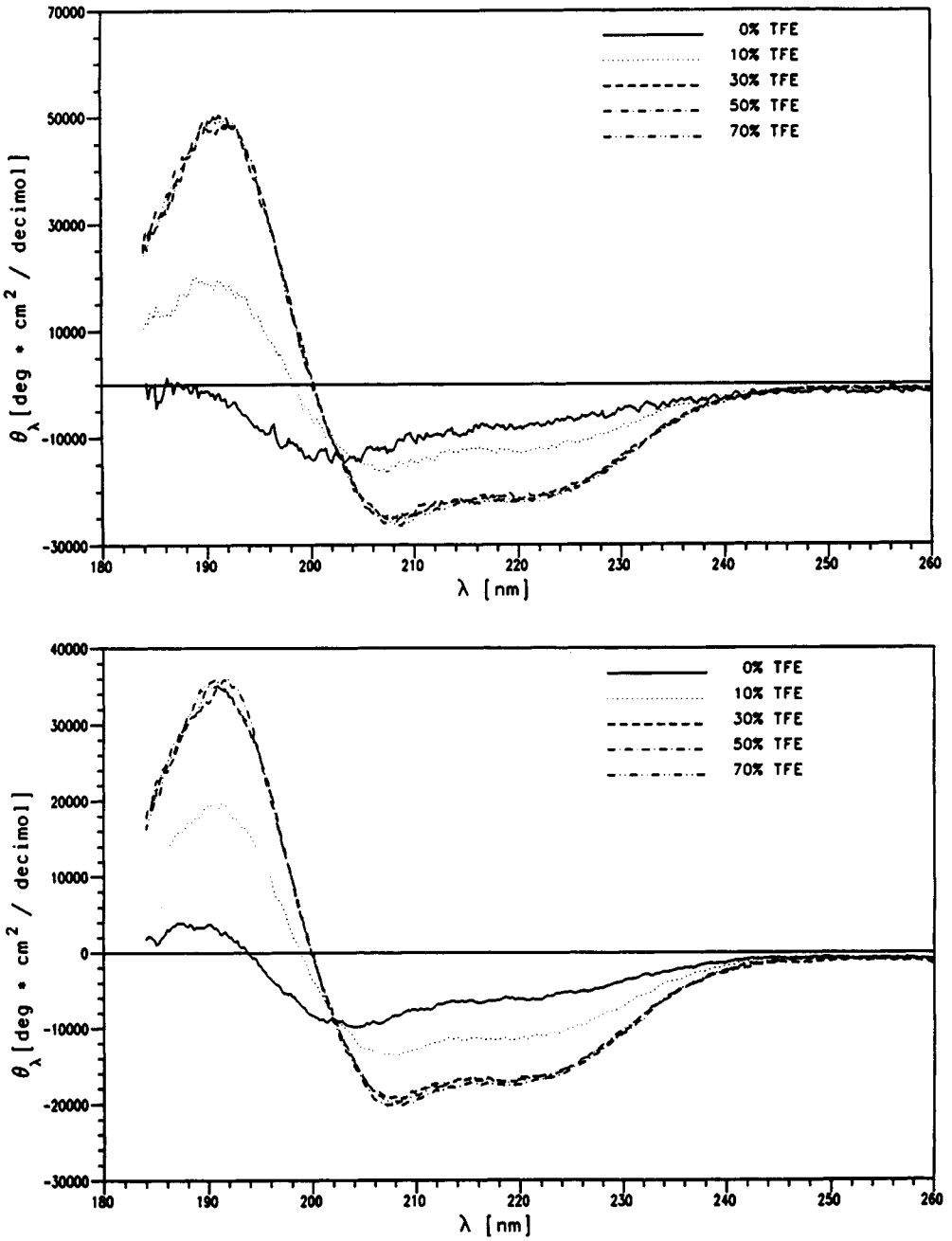

FIGURE 1: CD spectra of PACAP27 (upper) and PACAP38 (lower) in aqueous solution containing TFE.

Table I: Effect of TFE on the Secondary Structure Content of PACAP27 and PACAP38 Calculated by Deconvolution of CD Spectra with the Program VARSELEC

	PACAP27			PACAP38		
%TFE	α-helix	β-sheet	others	α-helix	β-sheet	others
0	15	20	65	20	21	59
10	36	13	51	37	15	48
30	66	5	29	53	9	38
50	71	2	27	55	8	37
70	67	4	29	54	10	36

ellipticity developing at 220 nm and a positive band at 191 nm. The helicity, calculated by the deconvolution program and shown in Table I, increased up to 30% TFE and, thereafter, remained constant for both peptides at 68% for PACAP27 and 54% for PACAP38. This corresponds to approximately 18 and 21 residues being involved in α-helical structures. Even in 0% TFE α-helical structures appear to be present in both peptides with approximately four and eight residues being involved, while any small amount of β-sheet present initially decreases on TFE addition.

Hence, in order to be in the region of maximum stable secondary structure, and as we were interested in determining the structure of the peptides in a hydrophobic environment, a solution of 1:1 (v/v) TFE/H_2O was choosen for studying the detailed molecular structure of the peptides in solution by NMR spectroscopy. The well-established strategy for structure determination of ^1H NMR spectroscopy was used (Wüthrich, 1986). Only the salient points are described here and are illustrated by reference to the spectra of PACAP27. Complete amino acid spin systems were readily identified from 2D ^1H phase-sensitive COSY and TOCSY spectra starting from the reasonably well resolved amide protons in the region 7.6 to 8.8 ppm (Figure 2). These were confirmed in the TOCSY spectra by inspection of the numerous cross peaks to high field corresponding to connectivities in the side chain. It was not found necessary to resort to recording data in fully deuterated solvents.

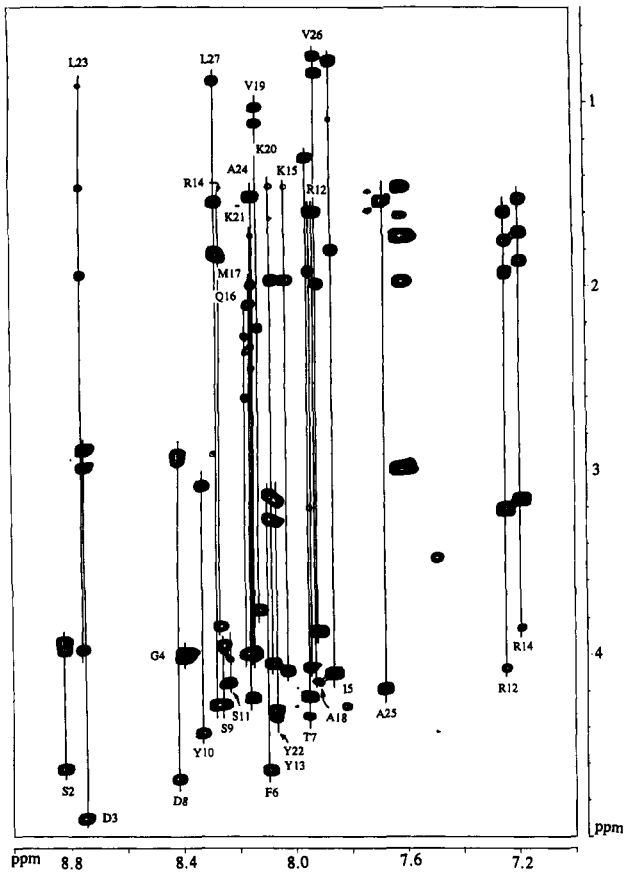

FIGURE 2: Part of a 2D CLEAN TOCSY spectrum (mixing time, 70 ms) of a 2 mM solution of PACAP27 in 1:1 (v/v) TFE-d_2/H_2O, pH 3.0 and 300 K, showing the amino acid spin systems.

Sequence-specific assignments were then determined using sequential NOE signals which reflect short distances between H_N, H_α, and H_β of amino acid i and H_N of amino acid i+1. Figure 3 shows consecutive strings of $d_{\alpha N}$ NOE's in the fingerprint region of the phase-sensitive NOESY spectrum showing the assignments from Ser-2 to Arg-14 and from Arg-14 to Leu-27, respectively. These assignments were confirmed by the $d_{\beta N}$ and d_{NN} connectivities of the same spectrum and are illustrated here by the latter connectivities, found in the amide region, for Phe-22 to Leu-27 (Figure 4). Lists of the chemical shift data for PACAP27 and PACAP38 are given in Tables II and III, respectively, and a summary of the NOE's is shown in Figures 5 and 6. In addition to the sequential NOE's, a considerable number of medium-range NOE's were now identified between H_α of residue i and H_N and H_β of residues i+3 and were indicative of α-helical interactions. In most cases these were initially found in the less crowded spectrum of PACAP27 and then readily identified in that of PACAP38. In most cases the relative intensities of these signals were the same in both spectra. Somewhat suprisingly this was true for the NOE's observed for residues at the end of the C-terminal region of PACAP27, where medium range NOE's were observed even to the terminal residue. Noteworthy are the readily observed $d_{NN}(i,i+2)$ (Figure 4) and $d_{\alpha N}(i,i+4)$ (Figure 3, lower) connectivities in this region, which confirm the presence of a stable helix to the chain end in PACAP27.

The α-proton chemical shift has been shown by several groups (Szilagyi & Jardetzky, 1989; Pastore & Saudek, 1990; Wishart et al., 1991) to be strongly dependent on the character and nature of protein secondary structure in a considerable number of proteins. For the 20 naturally occurring amino acids, the α-proton experiences an upfield shift with respect

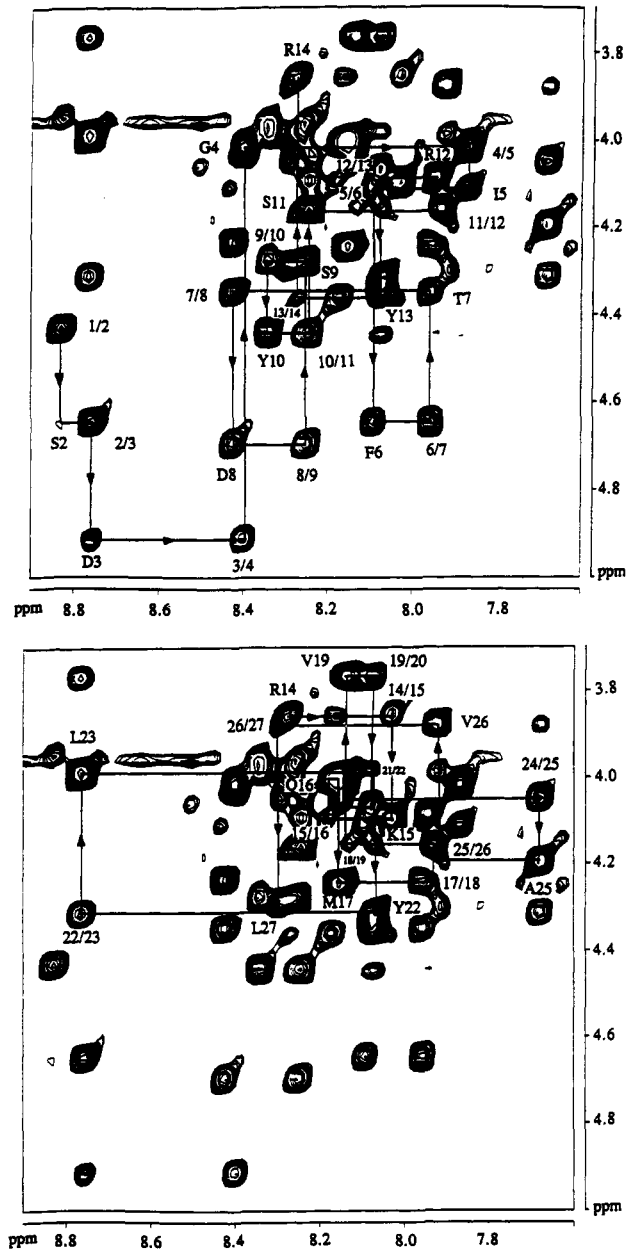

FIGURE 3: Fingerprint region of the 2D NOESY spectrum (mixing time, 150 ms) of PACAP27 showing the sequential assignments of the peptide: (upper) S2 to R14 and (lower) R-14 to L27. Solution conditions are as given in the legend to Figure 2.

to the random coil value in helices and a downfield shift in β-strands. This has led Wishart et al. (1992) to propose an empirical chemical shift index that affords a fast and simple method for the assessment of protein secondary structure. The importance of the method is that it affords a further reliable assessment of structure from data that already exist after signal assignments that is independent of the NOE structure determination. In practice, the α-protons are assigned an index of −1, 0, or 1 depending on whether they are shifted upfield by more than 0.1 ppm relative to the random value, are shift less than ±0.1 ppm, or are shifted downfield by more than 0.1 ppm, respectively. Secondary structure is attributed accordingly when a minimum number of indices are adjacent to one another (three for β-strand and four for α-helix). This analysis has been performed on both peptides using the data in Tables II and III to give the chemical shift index plots of Figure 7. Both peptides show an extended helix stretching from Ser-9 to Ala-25 in PACAP27 and to Val-26 in PACAP38, while a further helix is evident in the latter

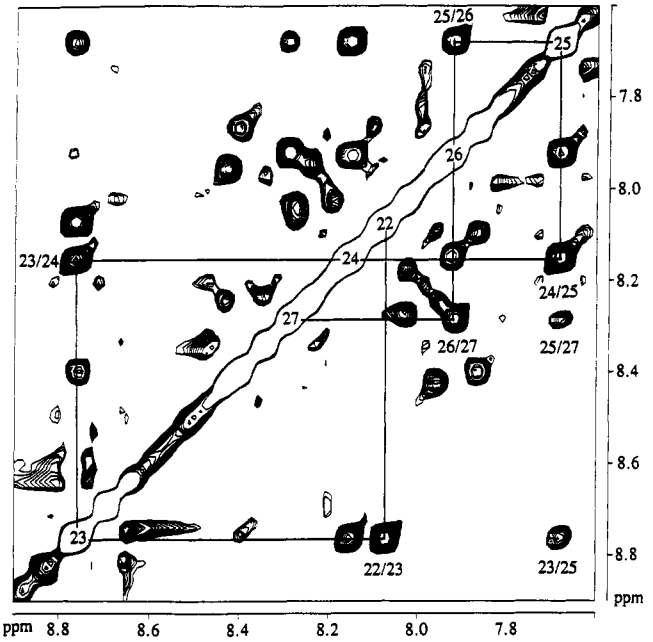

FIGURE 4: Same 2D NOESY spectrum as Figure 3 showing d_{NN} connectivities.

Table II: ^{1}H Assignment and Chemical Shift Data for PACAP-27 in Aqueous 50% TFE, pH 3.0, at 300 K

	NH	αH	βH	γH	δH	others
1 His		4.42	3.48			H-4, 7.49; H-2, 8.69
2 Ser	8.82	4.63	3.94, 3.98			
3 Asp	8.74	4.90	2.89, 2.98			
4 Gly	8.38	4.01, 4.03				
5 Ile	7.85	4.10	1.80	CH_2 1.10, 1.30 CH_3 0.79	0.79	
6 Phe	8.08	4.63	3.15, 3.28			H-2/6, 7.28; H-3-5, ~7.32
7 Thr	7.94	4.33	4.24	1.31		
8 Asp	8.41	4.68	2.94, 2.97			
9 Ser	8.24	4.26	3.96, 3.99			
10 Tyr	8.33	4.43	3.10			H-2/6, 7.15; H-3/5, 6.87
11 Ser	8.23	4.16	4.03, 4.09			
12 Arg	7.93	4.07	1.76, 1.94	1.61	3.21	NH, 7.24
13 Tyr	8.08	4.35	3.17			H-2/6, 7.06; H-3/5, 6.87
14 Arg	8.26	3.84	1.71, 1.86	1.53	3.15	NH, 7.19
15 Lys	8.01	4.10	1.98, 1.72	1.47	1.62	εH, 2.99; ϵNH_3^+, 7.61
16 Gln	8.17	4.00	2.12, 2.28	2.37, 2.61		$CONH_2$, 6.68, 7.01
17 Met	8.14	4.24	2.01, 2.11	2.33, 2.45		SCH_3, 2.20
18 Ala	7.91	4.15	1.59			
19 Val	8.12	3.76	2.24	1.03, 1.12		
20 Lys	8.07	4.05	1.99, 1.73	1.47	1.62	εH, 2.99; ϵNH_3^+, 7.61
21 Lys	8.15	3.97	2.00, 1.73	1.47	1.62	εH, 2.99; ϵNH_3^+, 7.61
22 Tyr	8.07	4.30	3.19			H-2/6, 7.09; H-3/5, 6.78
23 Leu	8.75	3.99	1.96, 2.03	1.48	0.93	
24 Ala	8.14	4.05	1.52			
25 Ala	7.67	4.19	1.53			
26 Val	7.91	3.86	1.99	0.76, 0.84		
27 Leu	8.28	4.29	1.82, 1.84	1.54	0.89	$CONH_2$, 6.85, 7.04

from Leu-29 to Arg-34. The N-terminus of both show no defined helix or strand structure.

After quantitation of the NOE data for PACAP27 (see Materials and Methods), 135 distance restraints, derived from the NOESY spectrum with a mixing time of 150 ms, were used to calculate 396 distance geometry structures of which four showed no restraint violations greater than 0.04 nm. Each

Table III: ^{1}H Assignment and Chemical Shift Data for PACAP-38 in Aqueous 50% TFE, pH 3.7, at 300 K

	NH	αH	βH	γH	δH	others
1 His		4.39	3.46			H-4, 7.47; H-2, 8.67
2 Ser	8.82	4.63	3.92, 3.97			
3 Asp	8.74	4.90	2.85, 2.95			
4 Gly	8.42	3.99, 4.04				
5 Ile	7.89	4.09		CH_2, 1.10, 1.30; CH_3, 0.78	0.78	
6 Phe	8.09	4.61	3.15, 3.26			H-2/6, 7.26; H-3-5, ~7.30
7 Thr	7.98	4.34	4.23	1.31		
8 Asp	8.43	4.66	2.87, 2.95			
9 Ser	8.27	4.25	3.92, 4.00			
10 Tyr	8.38	4.43	3.08			H-2/6, 7.11; H-3/5, 6.83
11 Ser	8.28	4.14	~4.00			
12 Arg	7.95	4.06	1.79, 1.93	1.59	3.21	NH, 7.29
13 Tyr	8.12	4.32	3.20			H-2/6, 7.03; H-3/5, 6.81
14 Arg	8.31	3.83	1.71, 1.85	1.49	3.13	NH, 7.19
15 Lys	8.04	4.10	1.99, 1.72	1.46	1.72	εH, 2.95; ϵNH_3^+, 7.61
16 Gln	8.19	4.00	2.12, 2.32	2.38, 2.64		$CONH_2$, 6.65, 7.00
17 Met	8.17	4.24	1.99, 2.12	2.32, 2.43		SCH_3, 2.27
18 Ala	7.98	4.23	1.61			
19 Val	8.15	3.76	2.24	1.04, 1.12		
20 Lys	8.19	4.00	2.01, 1.76	1.48	1.76	εH, 2.99; ϵNH_3^+, 7.61
21 Lys	7.89	4.06	2.01, 1.75	1.50	1.75	εH, 3.02; ϵNH_3^+, 7.61
22 Tyr	8.08	4.30	3.15, 3.26			H-2/6, 7.05; H-3/5, 6.74
23 Leu	8.87	3.97	1.94, 1.97	1.52	0.92	
24 Ala	8.29	4.05	1.53			
25 Ala	7.85	4.20	1.57			
26 Val	8.23	3.60	2.08	0.74, 0.88		
27 Leu	8.28	4.29	1.90	1.52	0.90	
28 Gly	8.19	3.91, 3.89				
29 Lys	7.91	4.17	2.01	1.50	1.75	εH, 3.02
30 Arg	8.13	4.14	1.79, 1.84	1.63	3.17	εH, 7.16
31 Tyr	8.42	4.33	3.15, 3.21			H-2/6, 7.08; H-3/5, 6.77
32 Lys	8.07	4.05	1.95	1.52	1.75	εH, 3.05
33 Gln	8.03	4.16	2.19	2.43, 2.54		$CONH_2$, 6.73, 7.39
34 Arg	7.98	4.24	1.76, 1.94	1.67	3.20	εH, 7.24
35 Val	7.90	3.95	2.08	0.90		
36 Lys	8.04	4.27	1.95	1.52	1.75	εH, 3.05
37 Asn	8.13	4.71	2.84, 2.89			$CONH_2$, 6.82, 7.57
38 Lys	8.08	4.31	1.88	1.52	1.75	$CONH_2$, 7.52, 6.97

of these was then subjected to the subsequent molecular dynamics refinement with two random velocity assignments per structure to give eight independent refined final structures. Inspection of these showed that various alignments of the final structures were possible. After an initial trial and error comparison, it was found that the structures could be aligned from Ser-9 to Val-26 (Figure 8, upper). RMS error analysis using all the backbone atoms of these residues and comparing each structure with every other structure (28 independent analyses) gave an average RMS deviation of 0.105 nm. Careful inspection of the structures showed, however, that this was improved if the molecule was independently aligned from Ser-9 to Lys-20 and from Lys-21 to Val-26 (Figure 8, middle and lower panels), when the average RMS deviation decreased to 0.065 and 0.049, respectively. In each case an α-helix is apparent. That a break exists in the helix between Lys-20 and Lys-21 is real and not an artifact of the calculations is, of course, apparent from an inspection of the NOE data. The cross peaks corresponding to NOE's $d_{\alpha N}(i,i+3)$ for residues 20–23 are very weak, as are those corresponding to

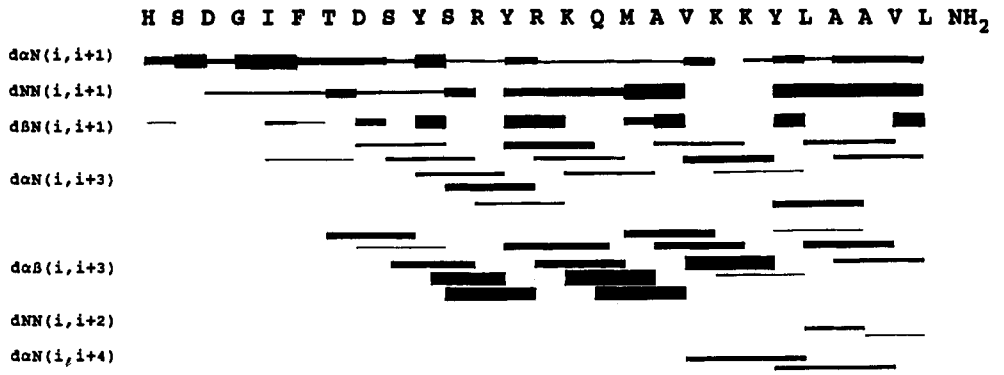

FIGURE 5: Summary of the observed NOE's for PACAP27. Solution conditions are as given in the legend to Figure 2.

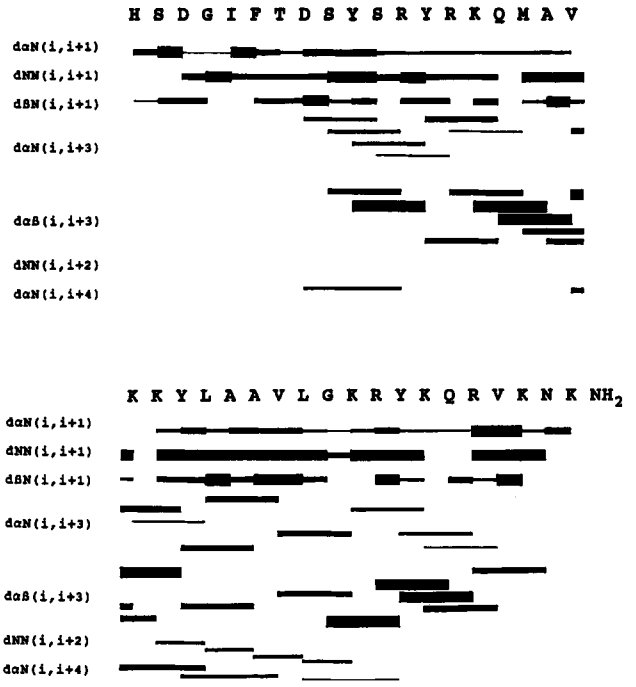

FIGURE 6: Summary of the observed NOE's for PACAP38. For solution conditions, see Table III.

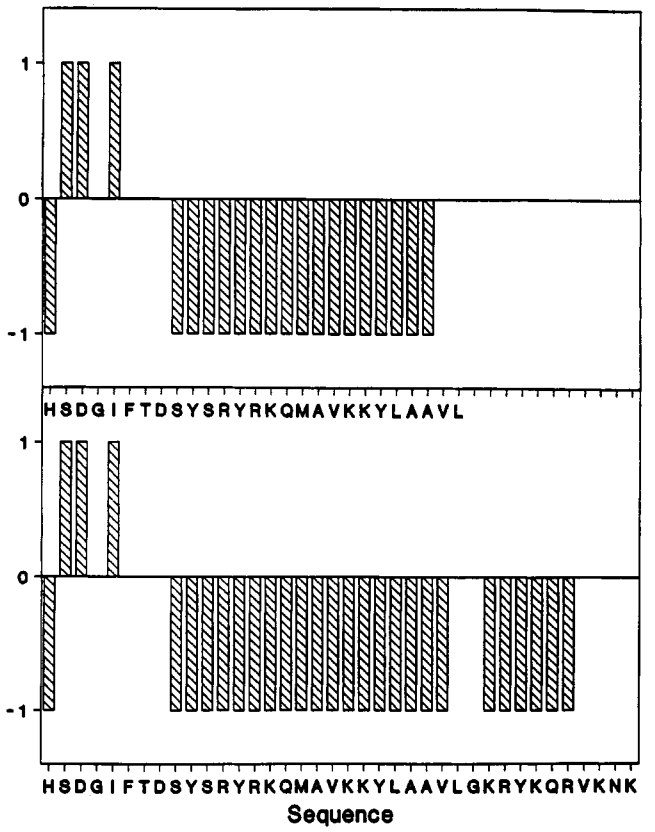

FIGURE 7: Chemical shift index of the α-protons of PACAP27 (upper) and PACAP38 (lower). Values were calculated from the data in Tables II and III and random coil values from Wishart et al. (1992).

$d_{\alpha\beta}(i,i+3)$ for residues 20–23 and 22–25, while the latter for residues 21–24 was absent.

Although for PACAP38 the overlap of signals restricted the number of observable NOE's 131 distance restraints were used, in an identical analysis to the above, to calculate 200 distance geometry structures. Five of these with restraint violations no greater than 0.10 nm were subsequently refined using several initial velocity assignments per structure to give 19 final refined structures. Again satisfactory alignments were found between Ser-9 and Lys-20, Lys-21 and Val-26, and Gly-28 and Arg-34 (Figure 9, upper, middle, and lower panels, respectively) with RMS deviations of 0.150, 0.110, and 0.075 nm, respectively. As with PACAP27, the same variation in the medium-range NOE cross peak intensities, involving residues 20–22, is observed, and the short non-structured region between Val-26 and Gly-28 is confirmed by the α-proton chemical shift data of Figure 7. The absence of any long-range NOE's between the side chains of the C-terminal helix and the other helices precludes any stable helix–helix interaction, nor are any observed between the disordered region and the rest of the molecule.

As expected from the chemical shift data, there is no evidence of α-helix or other stable structural features in the first eight N-terminal residues. This region appears to be able to access several conformations which, from the CD data, are not stabilized by higher concentrations of TFE.

DISCUSSION

As with numerous other investigations of short linear peptides, the 2D NOESY spectra show no evidence of stable structures for PACAP in aqueous solution. In contrast, however, the quantitative CD data indicate, even without TFE, that a number of residues are involved in α-helices which can only be rationalized by a transient involvement of a number of rapidly interconverting species. This is in keeping with the results from other small peptides, such as the N-terminal analogues of parathyroid hormone (Cohen et al., 1991). The change in the CD curve shows the appearance of a stable species with the transition being essentially complete at 30% TFE; further addition of TFE causes no increase in the number of residues involved in α-helical structures (Figure 1). The larger number of residues involved in the final structure of PACAP38 indicates the presence of α-helix in the C-terminal region, whose approximate position at Lys-29 to Arg-34 is delineated from the chemical shift index (Figure 7).

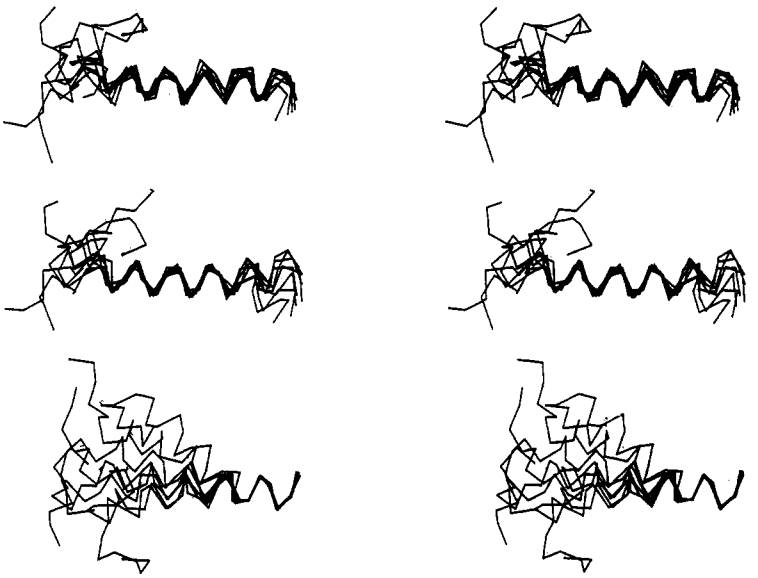

FIGURE 8: Stereoview superpositions of the eight final MD refined structures of PACAP27 after fitting of the backbone atoms C_α, C, and N of residues Ser-9 to Val-26 (upper), Ser-9 to Lys-20 (middle), and Lys-21 to Val-26 (lower).

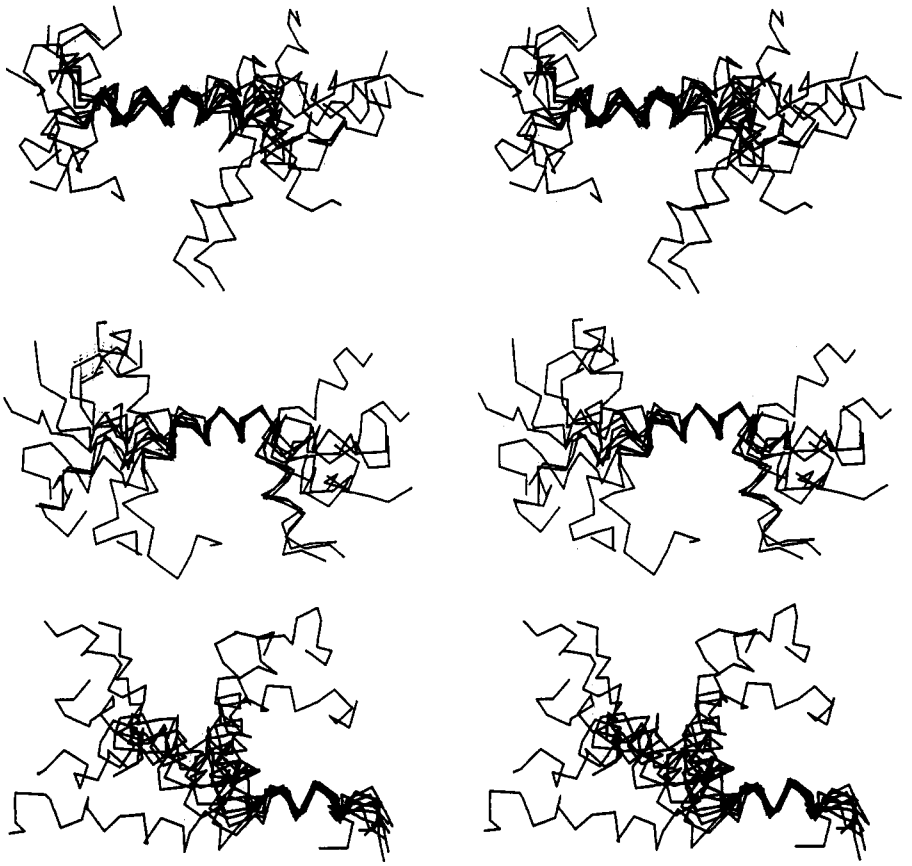

FIGURE 9: Stereoview superpositions of the ninteen final MD refined structures of PACAP38 after fitting of the backbone atoms C_α, C, and N of residues Ser-9 to Lys-20 (upper), Lys-21 to Val-26 (middle), and Gly-28 to Arg-34 (lower).

The number of residues involved in the α-helical structures, independently calculated from the CD (Table I) and chemical shift index data (Figure 7), is compatible with those found in the final refined structures calculated from the quantitative NOE data (PACAP27: 18, 17, and 18; PACAP38: 21, 24, and 25). The apparent observation of small amounts of β-sheet (Table I) in aqueous solution probably reflects the dynamic nature of the systems (Clore et al., 1986), as this is reduced to negligible amounts above 30% TFE.

The quantitative NOE data for PACAP27 resemble closely those of the appropriate N-terminal region of PACAP38, and as a consequence both structures in this region show a close correspondence. The somewhat poorer definition for PACAP38 must be attributed to the smaller number of distance constraints available for the structure calculations. In both structures, a break in the helix, stretching from Ser-9 to Val-26, between Lys-20 and Lys-21 is evident by improvements in the RMS deviation analyses. The C-terminal section from Lys-21 to Val-26, with the lower RMS deviation, is better defined and consequently less flexible than the one from Ser-9 to Lys-20. Quite remarkably, this second section extends to the peptide C-terminus without any loss of rigidity in the

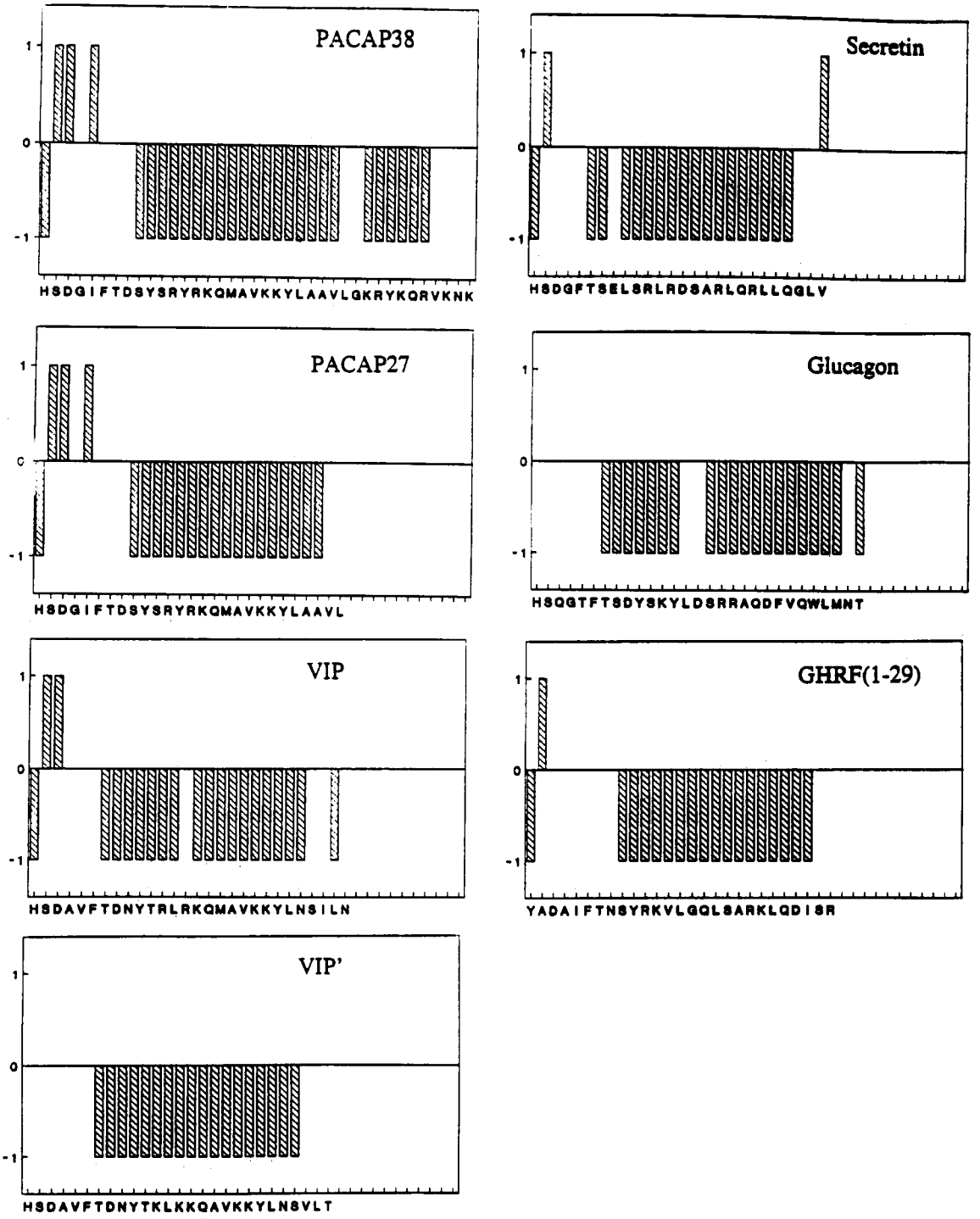

FIGURE 10: Comparison of the chemical shift indices of the α-protons of PACAP38 and PACAP27 in 50% TFE (present work), VIP in 40% TFE (Theriault et al., 1991), VIP' (Ac-[Lys-12, Lys-14, Nle-17, Val-26, Thr-28]VIP) in 50% methanol (Fry et al., 1989), secretin in 40% TFE (Gronenborn et al., 1987; Clore et al., 1988), glucagon in dodecylphosphocholine micelles (Braun et al., 1983), and GHRF(1–29) in 30% TFE (Clore et al., 1986) after normalization by correcting all the α-proton chemical shifts such that that of Phe-6 occurs at 4.63 ppm.

shorter peptide. For PACAP38 there is a flexible loop region between the end of this helix and the start of the well-defined C-terminal helix, which, in contrast to PACAP27, shows increased flexibility of the C-terminal residues.

Thus structurally PACAP38 has three well-defined domains: an initial disordered N-terminus of eight residues, followed by an extended α-helical region, consisting of two connected helices, and finally a C-terminal region with a short helix attached by a flexible hinge to the central domain. PACAP27 corresponds strictly to the first two domains. Defined as such, these three regions of PACAP38 are not only conformationally quite different, but there are also distinct differences in the nature of the amino acids present which impart quite different physical characteristics to the three domains. Thus the N-terminus is characterized by being the only domain to contain amino acids with negatively charged side chains and has only two with nonpolar side chains. The initial section (residues 9–16) of the middle domain contains no nonpolar amino acids, while these predominate (70%) in the second section, residues 17–26. The third domain contains a high percentage of positively charged and polar amino acids (eight out of 11).

The biological importance of the three domains can be gauged from the physiological data for the brain and peripheral organs that exist in the literature for several investigations with deletion and substitution analogues of PACAP. Thus

the initial domain is implicated in the activation of adenylate cyclase. In particular, the two N-terminal residues are necessary to stimulate relaxation of rat ileum (Clemens et al., 1992) and probably of guinea pig smooth muscle of the taenia caeci (Schwoerer et al., 1992), while several residues (1, 2, 3, 9, and 13) in the disordered domain and start of the first helix are important for high-affinity receptor binding in human SUP-T1 lymphoblastic membranes (Gourlet et al., 1991). The N-terminus is also necessary for the stimulation of rat pancreatic tumoral AR4-2J cell proliferation (Buscail et al., 1992) and glucose-induced insulin release (Mochizuki et al., 1992). Although the vasodilatory effects of various PACAP analogues on fermoral arterial blood flow are complex, analogues corresponding to the C-terminal region of PACAP38 caused increased flow at 1 nmol/kg levels, while those corresponding to the N-terminal domain (PACAP1–15) and middle domain (PACAP10–20) were without effect, and distinct differences between PACAP27 and PACAP38 were noted (Naruse et al., 1992). The C-terminal domain is also implicated in the differences found between the two peptides and their analogues in rat pancreatic cell membrane studies (Christophe et al., 1992a; Vandermeers et al., 1992). Last but not least, investigations of the structural requirements for the occupancy of rat brain PACAP receptors and adenylate cyclase activation by Robberecht et al. (1992) and Hou et al. (1992) conclude that three domains were important, namely, the N-terminal triplet His-Ser-Asp, the (14–26) area, and the C-terminal (27–38) extension, which are such that the presence intact of two of these suffices for high-affinity interactions at the binding level. The same group has also emphasized the importance of the lysines at positions 20 and 21, as combined substitution of these by glycine causes a sharp decrease in binding affinity of PACAP receptors in human neuroblastoma cell membranes (Christophe et al., 1992b; Robberecht et al., 1992).

Thus structural features attributable to the peptides in solution are of physiological importance, and even small irregularities in the helix make-up appear to be of significance. This is particularly encouraging and justifies further substitution studies, an area that has received considerable attention in protein design.

In more general terms, the structures found here resemble quite closely those of several related peptides. Gronenborn et al. (1987) have already noted the remarkable similarity of the structures of secretin, glucagon, and GHRF(1–29) under diverse solution conditions, and this can now be extended to include the PACAP and VIP peptides. These structural features are most graphically illustrated by comparison of the chemical shift indices (Figure 10), calculated for the various peptides from the reported α-proton chemical shifts, after normalization. There is always a disordered N-terminal region of 6–8 residues followed by an extended helical region of 19 $\pm$ 2 residues. The start of the helix is always at or near the highly conserved residues Phe-6 and Thr-7. In all cases, the hormones or neuropeptides show no stable structure in aqueous solution, and only on experiencing a hydrophobic environment, mimicked by TFE or micelles, is structure stabilized. It can be anticipated that further members of the family, such as helodermin (Naruse et al., 1986) and peptide histidine isoleucine (PHI), for which no NMR data are currently available, will also show these global features. In general, the primary active function of the hormones resides in the disordered region which presumably must have flexibility to adopt a specific conformation on the receptor, while it is tempting to ascribe the function of the helix as providing a suitable structure that can reside in the ordered lipid region surrounding the receptor site in the membrane. This structure is only assumed on transfer of the hormone from the dilute aqueous milieu to the hydrophobic environment of the membrane. The small differences in the detailed structure of the helical region, such as the presence of a half turn between residues 14 and 16 in secretin, glucagon, and GHRF(1–29) and irregularities in PACAP between 20 and 21, together with changes in the nature of the amino acid side chains, impart binding specificity to this region.

ADDENDUM

After submission of this paper, the structure of PACAP27 in 25% aqueous methanol was published (Inooka et al., 1992). This shows conformations similar to our structure in the region of residues 13–27 but has a significant difference for residues 9–12, where a β-turn-like conformation is suggested whereas we find α-helix. The qualitative data [$d_{\alpha\beta}(i,i+3)$ connectivities and H_α chemical shifts] found by Inooka et al. for these residues, however, appear to be more compatible with an α-helix conformation. The use of a limited NOE data set and a limited number of distance geometry calculations, without subsequent refinement with energy minimization and molecular dynamic calculations, may have led to a questionable end conformation.

ACKNOWLEDGMENT

We are grateful to T. Federau for help with the CD and chemical shift index programs.

REFERENCES

Arimura, A. (1992) *Regul. Pept. 37*, 287–303.
Braun, W., Wider, G., Lee, K. H., & Wüthrich, K. (1983) *J. Mol. Biol. 169*, 921–948.
Brünger, A. T., Clore, G. M., Gronenborn, A. M., & Karplus, M. (1986) *Proc. Natl. Acad. Sci. U.S.A. 83*, 3801–3805.
Buscail, L., Cambillau, C., Seva, C., Scemama, J. L., De Neef, P., Robberecht, P., Christophe, J., Susini, C., & Vaysse, N. (1992) *Gastroenterology 103*, 1002–1008.
Christophe, J., Vandermeers, A., Vandermeers-Piret, M.-C., Woussen-Colle, C., & Robberecht, P. (1992a) *Regul. Pept. 37*, 311.
Christophe, J., Vandermeers, A., Vandermeers-Piret, M.-C., Woussen-Colle, C., & Robberecht, P. (1992b) *Regul. Pept. 37*, 330.
Clemens, A., Katsoulis, S., Schwoerer, H., Creutzfeldt, W., & Schmidt, W. E. (1992) *Regul. Pept. 37*, 126.
Clore, G. M., Martin, S. R., & Gronenborn, A. M. (1986) *J. Mol. Biol. 191*, 553–561.
Clore, G. M., Nilges, M., Brünger, A., & Gronenborn, A. M. (1988) *Eur. J. Biochem. 171*, 479–484.
Cohen, F. E., Strewler, G. J., Bradley, M. S., Carlquist, M., Nilsson, M., Ericsson, M., Ciardelli, T. L., & Niessenson, R. A. (1991) *J. Biol. Chem. 266*, 1997–2004.
Fry, D. C., Madison, V. S., Bolin, D. R., Greeley, D. N., Toome, V., & Wegrzynski, B. B. (1989) *Biochemistry 28*, 2399–2409.
Gottschall, P. E., Tatsuno, I., & Arimura, A. (1991) *FASEB J. 5*, 194–199.
Gourlet, P., De Neef, P., Woussen-Colle, M.-C., Vandermeers, A., Vandermeers-Piret, M.-C., Robberecht, P., & Christophe, J. (1991) *Biochim. Biophys. Acta 1066*, 245–251.
Griesinger, C., Otting, G., Wüthrich, K., & Ernst, R. R. (1988) *J. Am. Chem. Soc. 110*, 7870–7872.
Gronenborn, A. M., Bovermann, G., & Clore, G. M. (1987) *FEBS Lett. 215*, 88–94.
Havel, T. F., & Wüthrich, K. (1984) *Bull. Math. Biol. 46*, 673–698.

Hennessey, J. P., & Johnson, W. C. (1981) *Biochemistry 20*, 1085–1094.
Hou, X., Robberecht, P., Vandermeers, A., Gourlet, P., Vandermeers-Piret, M.-C., & Christophe, J. (1992) *Regul. Pept. 37*, 170.
Inooka, H., Endo, S., Kitada, C., Mizuta, E., & Fujino, M. (1992) *Int. J. Pept. Protein Res. 40*, 456–464.
Jeener, J., Meier, B. H., Bachmann, P., & Ernst, R. R. (1979) *J. Chem. Phys. 71*, 4546–4553.
Johnson, W. C. (1990) *Proteins 7*, 205–214.
Macura, S., Huang, Y., Sutter, D., & Ernst, R. R. (1981) *J. Magn. Reson. 43*, 259–281.
Mammi, S., & Peggion, E. (1990) *Biochemistry 29*, 5265–5269.
Miyata, A., Arimura, A., Dahl, R. R., Minamino, N., Uehara, A., Jiang, L., Culler, M. D., & Coy, D. H. (1989) *Biochem. Biophys. Res. Commun. 164*, 567–574.
Mochizuki, T., Takatsuka, N., Ohshima, K., Sato, K., Kakuyama, H., & Yanaihara, N. (1992) *Regul. Pept. 40*, 211.
Motta, A., Pastore, A., Goud, N. A., & Castiglione Morelli, M. A. (1991) *Biochemistry 30*, 10444–10450.
Naruse, S., Yashi, A., Kishida, S., Kadowaki, M., Hoshino, M., Ozaki, T., Robberecht, P., Christophe, J., Yanaihara, C., & Yanaihara, N. (1986) *Peptides 7*, 237–240.
Naruse, S., Ozaki, T., & Nokihara, K. (1992) *Regul. Pept. 40*, 214.
Neidig, K.-P., & Kalbitzer, H. R. (1990) *J. Magn. Reson. 88*, 155–160.
Nokihara, K., Naruse, S., & Wray, V. (1991) *Pept. Chem.* 13.
Nokihara, K., Naruse, S., Ando, E., & Wray, V. (1992) in *Peptides 1992* (Schneider, C. H., & Eberle, A. N., Eds.) ESCOM, Leiden, The Netherlands.
Pastore, A., & Saudek, V. (1990) *J. Magn. Reson. 90*, 165–176.
Rance, M., Sorensen, O. W., Bodenhausen, G., Wagner, G., Ernst, R. R., & Wüthrich, K. (1983) *Biochem. Biophys. Res. Commun. 117*, 479–485.
Redfield, A., & Kunz, S. D. (1975) *J. Magn. Reson. 19*, 250–254.
Robberecht, P., Gourlet, P., De Neef, P., Woussen-Colle, M.-C., Vandermeers-Piret, M.-C., Vandermeers, A., & Christophe, J. (1992) *Eur. J. Biochem. 207*, 239–246.
Salomon, R., Couvineau, A., Rouyer-Fessard, C., Voisin, T., Lavallee, D., Blais, A., Darmoul, D., & Laburthe, M. (1992) *Regul. Pept. 40*, 242.
Schwoerer, H., Katsoulis, S., Creutzfeldt, W., & Schmidt, W. E. (1992) *Regul. Pept. 40*, 248.
Schomburg, D., & Reichelt, J. (1988) *J. Mol. Graphics 6*, 161–165.
Schwyzer, R. (1986) *Biochemistry 25*, 6335–6342.
Sönnichsen, F. D., Van Eyk, J. E., Hodges, R. S., & Sykes, B. D. (1992) *Biochemistry 31*, 8790–8798.
Szilagyi, L., & Jardetzky, O. (1989) *J. Magn. Reson. 83*, 441–449.
Theriault, Y., Boulanger, Y., & St-Pierre, S. (1991) *Biopolymers 31*, 459–64.
Vandermeers, A., Vandenborre, S., Hou, X., De Neef, P., Robberecht, P., Vandermeers-Piret, M.-C., & Christophe, J. (1992) *Regul. Pept. 40*, 266.
Wishart, D. S., Sykes, B. D., & Richards, F. M. (1991) *J. Mol. Biol. 222*, 311–333.
Wishart, D. S., Sykes, B. D., & Richards, F. M. (1992) *Biochemistry 31*, 1647–1651.
Wüthrich, K. (1986) *NMR of Proteins and Nucleic Acids*, Wiley-Interscience, New York.
Zuiderweg, E. R. P., Hallenga, K., & Olejniczak, E. T. (1986) *J. Magn. Reson. 70*, 336–343.